Int. J. Electrochem. Sci., 8 **(2013)** 7816 - 7824

International Journal of
ELECTROCHEMICAL
SCIENCE
www.electrochemsci.org

Short Communication

High Rate Capability of Nd-Doped $Li_4Ti_5O_{12}$ as an Effective Anode Material for Lithium-Ion Battery

Qianyu Zhang, Xi Li[*]

Department of Environmental Science and Engineering, Fudan University, Shanghai 200433, China
[*]E-mail: xi_li@fudan.edu.cn

Received: 23 April 2013 / *Accepted:* 14 May 2013 / *Published:* 1 June 2013

Nd doped $Li_4Ti_5O_{12}$ (LTO) was synthesized by a sol-gel method. The structure and electrochemical properties of the as-prepared powders were systematically investigated. $Li_4Ti_{4.98}Nd_{0.02}O_{12}$ exhibits excellent rate capabilities and cycling stability even at a high current rate of 10 C. Particularly, even without utilizing carbon black as conductive material, the $Li_4Ti_{4.98}Nd_{0.02}O_{12}$ still shows outstanding rate capability and cyclability at a rate of 5 C. The excellent high rate performance may be ascribed to the increased lattice constant and improved electronic conductivity resulting from the Nd-doping. The novel $Li_4Ti_{4.98}Nd_{0.02}O_{12}$ material stands as a promising potentially high rate anode material to be used in power lithium-ion battery.

Keywords: Lithium-ion batteries; Anode materials; $Li_4Ti_5O_{12}$; Doping; High rate capability

1. INTRODUCTION

Lithium ion batteries (LIBs) are nowadays widely used as power sources for various electronic devices due to their high energy density and long cycle life [1]. However, there have always been safety issues arising from the dendritic lithium ion growth on the anode surface at high charging current because the conventional carbon materials approach almost 0 V (vs. Li/Li^+) at the end of Li insertion [2-3]. Recently, the spinel LTO has been demonstrated as a potential substitute for the graphite anode in LIBs because of its higher flat operating voltage of about 1.5 V (vs. Li/Li^+) that can avoid the safety problem caused by the deposition of metallic Li [4]. Besides, LTO is a so called zero-strain insertion material that accommodates Li with a theoretical capacity of 175 $mAh \cdot g^{-1}$ [5]. Although it has many advantages, it cannot meet the need of practical application owing to its poor electronic conductivity with associated poor charge-discharge properties at high current rates [6].

Several strategies have been taken to solve this problem, including synthesizing the nanosized particles [7-10], doping with metal ions or non-metal ions [11-17] and coating with a conductive second phase such as carbon, Ag and polyacene [18-20]. Synthesizing nanosized LTO particles and coating with conductive phase can somehow improve the rate capability. However, the rate capabilities are still unsatisfactory and can not meet the demand for high power density. In fact, decreasing the LTO particle size to the nanoscale results in an anode with very low power tap density, which significantly decrease the volumetric density of LIB. Coating carbon on the surface or compositing with carbon materials could not enhance the intrinsic electronic and Li ionic conductivities, which inside the LTO particles are still poor. According to some recent research, rare earth doping could improve the cycling performance and high rate capability [21-23]. However, up to now, no investigation has been reported on the Nd-doped LTO (NLTO) as an anode material for LIBs.

As has been reported, doping $LiMn_2O_4$ with lower valence cation Nd^{3+} yields oxygen ion vacancies, which could behave as ionic charge carriers to greatly enhance the electronic conductivity of $LiMn_2O_4$ [24]. Inspired by this work, we prepared LTO with various Nd-doping contents, and systematically investigated its high rate performance. This material has clearly demonstrated an excellent improvement in high rate capability and cyclability in LIB.

2. EXPERIMENTAL

2.1 Synthesis and characterization of the samples

All the reagents involved in the present work are analytically pure. The preparation of NLTO includes four steps. (1) 17 g tetrabutyl titanate (TBT) was added into 20 mL ethanol to form solution A, 2.52 g $LiOH{\cdot}2H_2O$ and an appropriate amount of $Nd(OOCCH_3)_3{\cdot}XH_2O$ were dissolved in deionized water to form solution B. (2) Solution A was titrated into solution B under magnetic stirring. (3) The mixture was dried at 100 ℃ thoroughly. (4) The dried mixture was calcined at 750 ℃ for 10 h. To obtain N_xLTO (x=0, 0.01, 0.02 and 0.03), the weight of $Nd(OOCCH_3)_3{\cdot}XH_2O$ added was 0, 0.032, 0.064 and 0.096 g, respectively. The crystal structure of the as-prepared samples was identified by XRD using Cu-Kα radiation ($10^o \leq 2\theta \leq 80^o$).

2.2 Battery preparation and electrochemical measurement

The electrochemical characteristics were evaluated by means of two-electrode CR2032 coin cells. The sample slurry was prepared by mixing active material powders with conductive carbon (acetylene black) and binder (PVDF) at a weight ratio of 82:10:8 in N-methyl-2-pyrrolidine (NMP). Subsequently, the slurry was coated on a copper foil using the doctor blade technique and dried at 120 ℃ for 10 h to evaporate the NMP solvent. The electrode foil was punched to 12 mm diameter discs, which were used to assemble the coin cells in an Ar glove box where both moisture and oxygen content were less than 1ppm. Li foil was used as the counter and reference electrode in the cell. Celgard 2400 was the separator. The electrolyte solution was 1 M LiPF6 dissolved in a 1:1:1 mixture

by volume of ethlylene carbonate (EC), dimethyl carbonate (DMC), ethylmethyl carbonate (EMC). The performance of the cells was evaluated galvanostatically in the voltage range of 1-2.5 V (*vs.* Li/Li^+) at various current rates with a relaxation time of 1 min between charge and discharge unless otherwise indicated.

3. RESULTS AND DISCUSSION

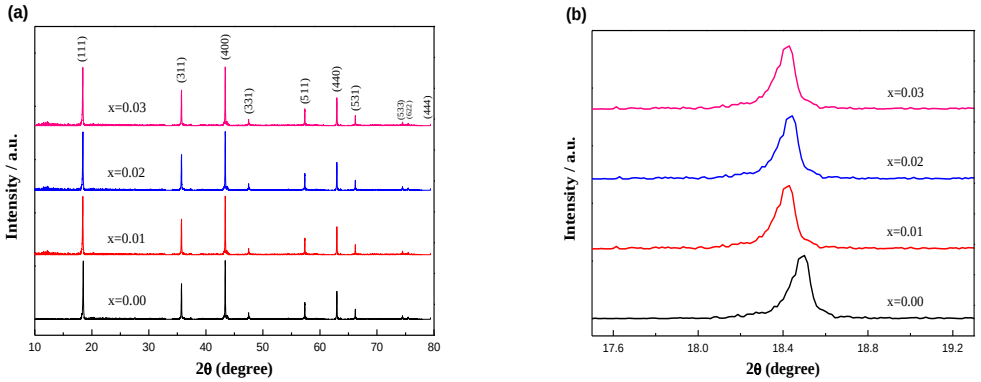

Figure 1. (a) XRD patterns and (b) enlarged (111) peaks of N_xLTO (x= 0, 0.01, 0.02 and 0.03) samples.

The XRD patterns of NLTO with various Nd-doping contents are shown in Fig. 1(a). The diffraction peaks of all samples can be indexed as cubic spinel LTO. No impurity peaks can be detected, indicating that the small amount of Nd^{3+} has entered the lattice structure of LTO without any structure changes. For clear observation, the peak positions of (1 1 1) planes of the samples are magnified and shown in Fig. 1(b). The lattice parameters of the samples obtained according to the Rietveld method are shown in Table 1. It can be observed that the lattice parameter increases with the increased amount of Nd-doping. The increased lattice constant resulting from Nd-doping could broaden the pathway for Li ion diffusion and enhance the diffusion coefficient, thus is conducive to the insertion/extraction of Li ions.

Table 1. Lattice parameters of synthesized NxLTO samples doped with different Nd amount: x=0, 0.01, 0.02, 0.03.

Sample	a (Å)
x=0.00	8.348
x=0.01	8.351
x=0.02	8.353
x=0.03	8.357

High rate performance is an important requirement for power LIBs. To demonstrate the effect

of Nd-doping on improving the rate capability of the electrodes, the rate performance of the N_xLTO ($0 \leq x \leq 0.03$) samples at different current rates is shown in Fig. 2. For each stage the charge-discharge processes of the samples were taken for 10 cycles.

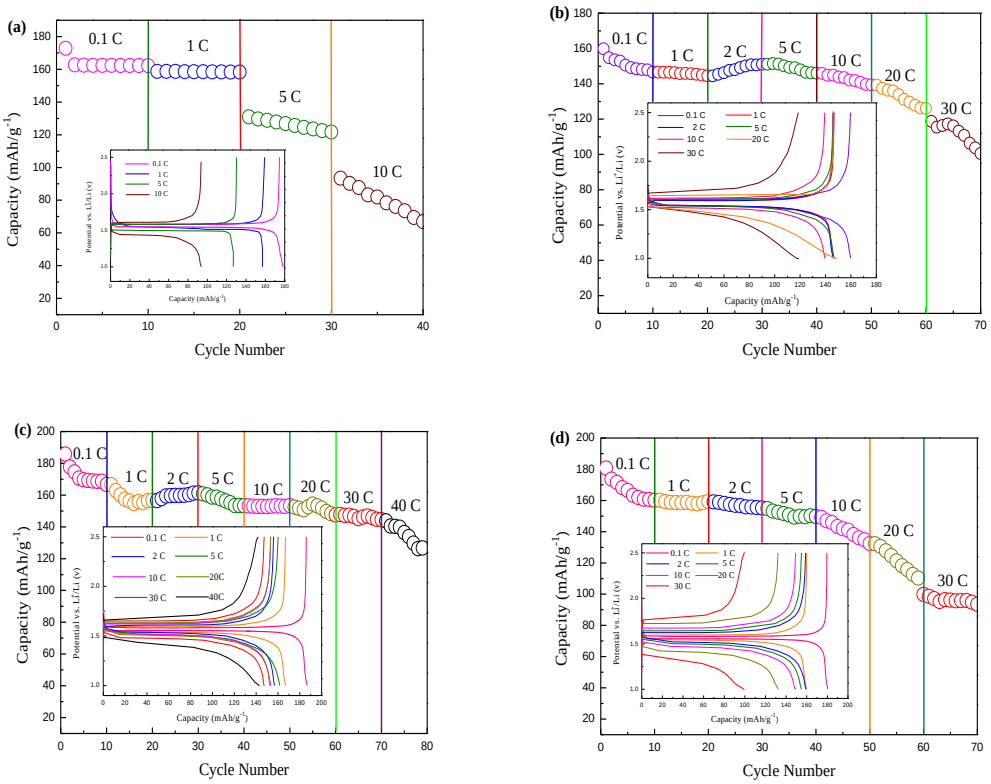

Figure 2. Rate capabilities of NxLTO for x=0 (a), 0.01 (b), 0.02 (c) and 0.03 (d). The insets are the corresponding charge-discharge curves of the first cycle at various rates.

Table 2. Comparison of rate performances for various metallic ion-doped LTO.

Samples	Synthesis method	Discharge current	Capacity ($mAh \cdot g^{-1}$)	Reference
$N_{0.02}LTO$	Sol-gel	10 C	147.6	Current study
$Li_{3.5}Zn_{0.5}Ti_5O_{12}$	Solid-state	4 C	108	[25]
$Li_4Ti_{4.8}Zn_{0.2}O_{12}$	Solid-state	5 C	180	[26]
$Li_4Ti_{4.9}Zr_{0.1}O_{12}$	Solid-state	20 C	118	[27]
$Li_4Ru_{0.01}Ti_{4.99}O_{12}/C$	Solid-state	10 C	110	[28]
$Li_4Ti_{4.95}Nb_{0.05}O_{12}$	Sol-gel	20 C	127	[29]
$Li_4Ti_{4.9}V_{0.1}O_{12}$	Solid-state	5 C	117.3	[30]
$Li_4Ti_{4.95}Ta_{0.05}O_{12}$	Solid-state	10 C	116.1	[31]
$Li_4Ti_{4.95}AI_{0.05}O_{12}$	Sol-gel	5 C	116	[32]
$Y_{0.06}LTO$	Sol-gel	10 C	161.1	[33]
$Li_{3.9}Sn_{0.1}Ti_5O_{12}/C$	Sol-gel	5 C	130	[34]
$Li_4Ti_{4.8}Ni_{0.1}Mn_{0.1}O_{12}$	Sol-gel	0.5 C	172.41	[11]
$Li_{0.35}La_{0.55}TiO_3$	Sol-gel	5 C	150.79	[23]

From Fig. 2a, the reversible capacity of pure LTO decreases markedly with increasing the current rate from 0.1 to 10 C. For Nd-doping contents of 0.01-0.03, $N_{0.02}$LTO exhibits excellent rate performance even when cycled at a rate of 40 C (Fig. 2c). However, when the Nd-doping content reaches 0.03, the rate performance worsens, demonstrative of over doping of Nd in LTO. It can be clearly seen that $N_{0.02}$LTO presents the best rate performance among the samples.

Table 2 compares the results of the current study with the rate capability taken from the literature for various metallic ion-doped LTO electrodes discharge to 1 V. It demonstrates that the rate performance of $N_{0.02}$LTO obtained in this study is considered highly comparable or even much better than the majority of LTO anodes.

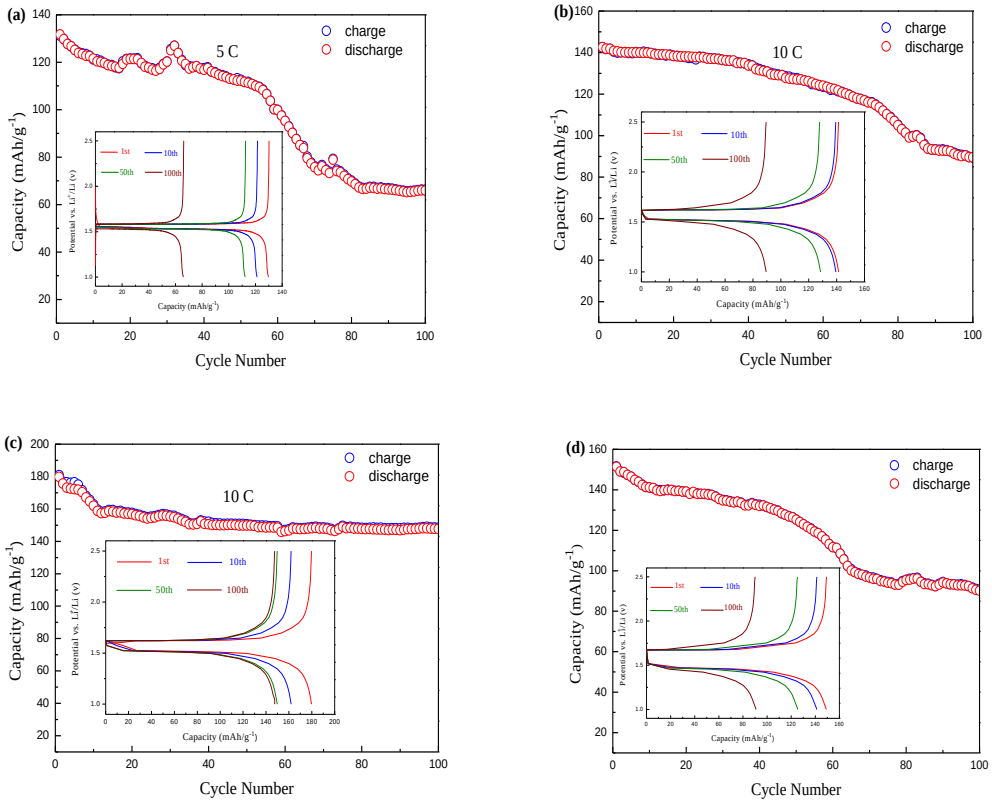

Figure 3. Cyclic performance of NxLTO for x=0 (a), 0.01 (b), 0.02 (c) and 0.03 (d). The insets are the corresponding charge-discharge curves of selected cycles.

The corresponding charge-discharge curves of the first cycle at various rates are depicted in the insets of Fig. 2, further demonstrating the dependence of the rate performance on the Nd-doping content in LTO.

To evaluate the cycling stability of the as-prepared samples, the cycling performances of LTO electrode at 5 C and Nd-doped LTO electrodes at 10 C are shown in Fig. 3. The reversible capacity of LTO decreases almost linearly to 65.9 mAh·g^{-1} when cycled at 5 C for 100 cycles (shown in Fig. 3a). With respect to N_xLTO cycled at 10 C after 100 cycles, the reversible capacities are 89.5 mAh·g^{-1} for x=0.01 (Fig. 3b), 147.6 mAh·g^{-1} for x=0.02 (Fig. 3c) and 90.1 mAh·g^{-1} for x=0.03 (Fig. 3d), which are

more stable than that of undoped LTO. Thus, $N_{0.02}$LTO exhibits the highest capacity among all samples. From the corresponding charge-discharge curves for selected cycles shown in the insets of Fig. 3, the reaction mechanism does not alter during the cycling process. Taking into consideration the cyclability and rate capability, $N_{0.02}$LTO demonstrates optimal comprehensive performance.

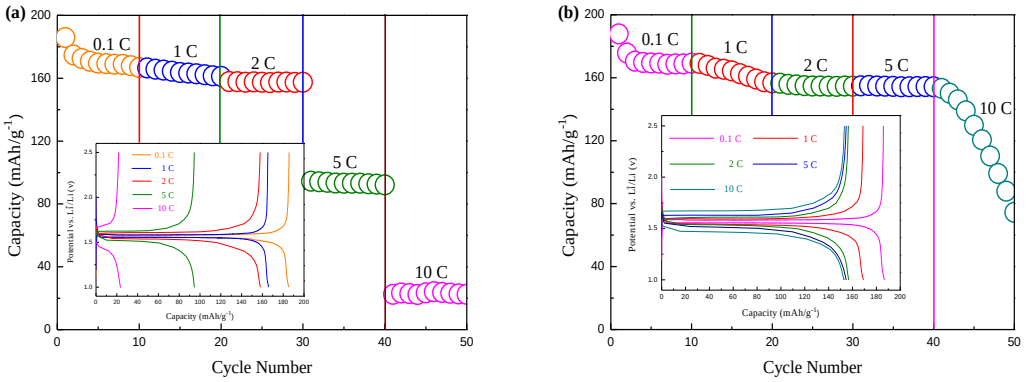

Figure 4. Rate performance of LTO (a) and $N_{0.02}$LTO (b) without using carbon black as conductive material. The insets are the first charge-discharge curves at various rates.

An comparative test was used to experimentally verify the improved electronic and ionic conductivities of NLTO. No carbon black was added in the slurry and the weight ratio of LTO or $N_{0.02}$LTO to polyvinylidene fluoride is 9:1 when fabricating the electrodes. The rate capabilities of LTO and $N_{0.02}$LTO without conductive materials are shown in Fig. 4. Even in the absence of carbon black, the $N_{0.02}$LTO cell could still maintain a stable reversible capacity of 154.3 $mAh \cdot g^{-1}$ at a rate of 5 C, and the capacities at 1, 2 and 5 C exhibit almost no reduction. The rate performance of the $N_{0.02}$LTO cell is obviously superior to that of LTO using carbon black as conductive material (Fig. 2a), and is significantly enhanced over that of LTO cell without conductive carbon black at identical rates (Fig. 4a).

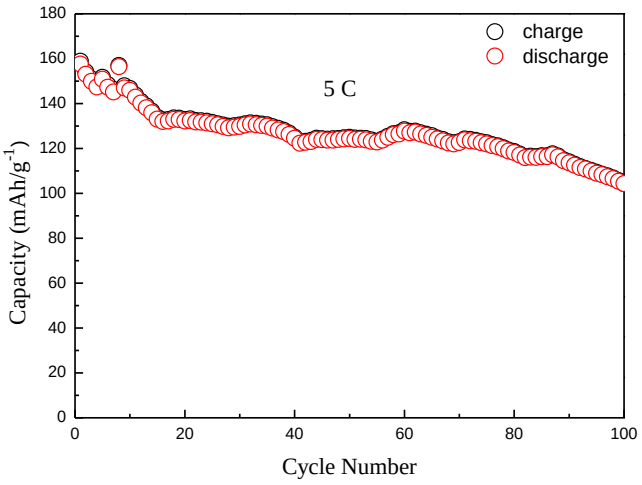

Figure 5. The cycling performance of the $N_{0.02}$LTO cell without using carbon black as conductive material at 5 C rate. The inset is the curves for selected cycles.

The cycling performance of the $N_{0.02}$LTO cell without the addition of carbon black was also tested at 5 C (Fig. 5). The reversible capacity is 104.3 mAh·g^{-1} after 100 cycles, which is also much higher than that of the LTO cell using carbon black as conductive material (Fig. 3a). These indicate that the Nd-doped LTO really possesses good electronic and ionic conductivities, which are beneficial for the high rate performance of LIBs.

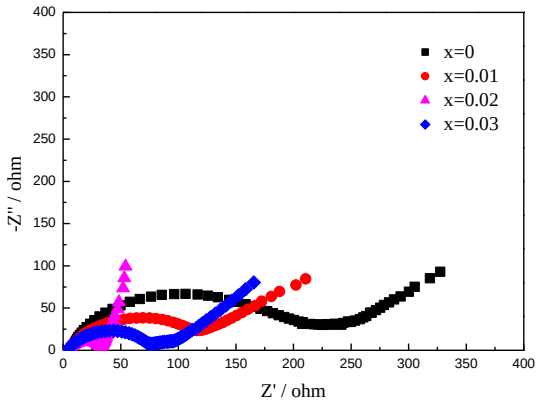

Figure 6. AC impedance spectra of NxLTO (x= 0, 0.01, 0.02 and 0.03) electrodes.

Fig. 6 shows the AC impedance spectra of LTO and Nd-doped LTO electrodes. The EIS measurements were carried out after the cells were charge-discharged by one cycle at the stable voltage of 1.55 V (vs. Li/Li$^+$). All the EIS curves are composed of a depressed semicircle at the high to intermediate frequency range, and there is a straight line at lowest frequency region. The high frequency semicircle is related to the charge transfer resistance at the active material interface, while the sloping line at the low frequency end indicates the Warburg impedance caused by a semi-infinite diffusion of Li$^+$ ion in the electrode. It can be found from the Fig. 6 that the charge transfer resistance of $N_{0.02}$LTO is much lower than that of other samples. The decrease of charge transfer resistance is beneficial to the improvement in conductivity and the kinetic behaviors during charge-discharge process, which is attributed to the doping of Nd^{3+} in LTO. The EIS results demonstrate that $N_{0.02}$LTO electrode would have the best high rate performance.

4. CONCLUSION

NLTO with different Nd-doping contents was prepared by a sol-gel method. XRD results show that the dopant Nd thoroughly entered the lattice structure of LTO as the doping amount increased, and no impurity was detected. The electrochemical reaction process has not been changed by Nd doping, as indicated by charge-discharge curves at various current rates. EIS results indicate that the conductiv-ity is improved by Nd doping and, hence, an improvement in rate capability is achieved. $N_{0.02}$LTO exhibited the best high rate capability and cyclability among all samples. Even when directly cycled at a current rate of 10 C without carbon black as conductive material, an outstanding cyclic performance

can still be achieved. All evidences demonstrate that Nd-doped LTO could be a promising anode material for high rate LIBs.

ACKNOWLEDGMENTS

This work was supported by National Natural Science Foundation of China (No. 61171008, 21103024), Shanghai Pujiang Rencai Project (No. 09PJ1401400), and the funds from Dalian Mingjia Jinshu Products Limited Company and Suzhou Baotan New Energy Limited Company.

References

1. M. Armand and J.M. Tarascon, *Nature*, 451 (2008) 652.
2. Q.Y. Zhang, C.C. Qiu, Y.B. Fu and X.H. Ma, *Chin. J. Chem.*, 27 (2009) 1459.
3. Q.Y. Zhang, Y.T. Zhang, C.C. Qiu, Y.B. Fu and X.H. Ma, *Acta Chim. Sinica*, 67 (2009) 1713.
4. G.N. Zhu, Y.G. Wang and Y.Y. Xia, *Energy Environ. Sci.*, 5 (2012) 6652.
5. Q.Y. Zhang and X. Li, *Int. J. Electrochem. Sci.*, 8 **(**2013**)** 6449.
6. S.H. Huang, Z.Y. Wen, X.J. Zhu and Z.H. Gu, *Electrochem. Commun.*, 6 (2004) 1093.
7. K. Nakahara, R. Nakajima, T. Matsushima and H. Majima, *J. Power Sources*, 117 (2003) 131.
8. H.F. Ni and L.Z. Fan, *J. Power Sources*, 214 (2012) 195.
9. Y.S. Lin, M.C. Tsai and J.G. Duh, *J. Power Sources*, 214 (2012) 314.
10. Y.J. Hao, Q.Y. Lai, Z.H. Xu, X.Q. Liu and X.Y. Ji, *Solid State Ionics*, 176 (2005) 1201.
11. W.M. Long, X.Y. Wang, S.Y. Yang, H.B. Shu, Q. Wu, Y.S. Bai and L. Bai, *Mater. Chem. Phys.*, 131 (2011) 431.
12. A.D. Robertson, L. Trevino, H. Tukamoto and J.T.S. Irvine, *J. Power Sources*, 81–82 (1999) 352.
13. Y.J. Hao, Q.Y. Lai, J.Z. Lu and X.Y. Ji, *Ionics*, 13 (2007) 369.
14. J. Gao, J.R. Ying, C.Y. Jiang and C.R. Wan, *Ionics*, 15 (2009) 597.
15. T.F. Yi, Y. Xie, J. Shu, Z.H. Wang, C.B. Yue, R.S. Zhu and H.B. Qiao, *J. Electrochem. Soc.*, 158 (2011) A266.
16. Q.Y. Zhang, C.L. Zhang, B. Li, S.F. Kang, X. Li and Y.G. Wang, *Electrochim. Acta*, 98 (2013) 146.
17. H.B. Wu, S. Chang, X.L. Liu, L.Q. Yu, G.L. Wang, D.X. Cao, Y.M. Zhang, B.F. Yang and P.L. She, *Solid State Ionics*, 232 (2013) 13.
18. T. Yuan, X. Yu, R. Cai, Y.K. Zhou and Z.P. Shao, *J. Power Sources*, 195 (2010) 4997.
19. P.C. Chen, M.C. Tsai, H.C. Chen, I.N. Lin, H.S. Sheu, Y.S. Lin, J.G. Duh, H.T. Chiu and C.Y. Lee, *J. Mater. Chem.*, 22 (2012) 5349.
20. G.Y. Liu, H.Y. Wang, G.Q. Liu, Z.Z. Yang, B. Jin and Q.C. Jiang, *Electrochim. Acta*, 87 (2013) 218.
21. T.F. Yi, B. Chen, H.Y. Shen, R.S. Zhu, A.N. Zhou and H.B. Qiao, *J. Alloys Compd.*, 558 (2013) 11.
22. C.X. Qiu, Z.Z. Yuan, L. Liu, N. Ye and J.C. Liu, *J. Solid State Electrochem.*, 17 (2013) 841.
23. W. Wang, H.L. Wang, S.B. Wang, Y.J. Hu, Q.X. Tian and S.Q. Jiao, *J. Power Sources*, 228 (2013) 244.
24. R. Singhal, S.R. Das, M.S. Tomar, O. Ovideo, S. Nieto, R.E. Melgarejo and R.S. Katiyar, *J. Power Sources*, 164 (2007) 857.
25. B. Zhang, H.D. Du, B.H. Li and F.Y. Kang, *Electrochem. Solid State Lett.*, 13 (2010) A36.
26. T.F. Yi, H.P. Liu, Y.R. Zhu, L.J. Jiang, Y. Xie and R.S. Zhu, *J. Power Sources*, 215 (2012) 258.
27. X. Li, M.Z. Qu and Z.L. Yu, *J. Alloys Compd.*, 487 (2009) L12.
28. C.Y. Lin, Y.R. Jhan and J.G. Duh, *J. Alloys Compd.*, 509 (2011) 6965.
29. B.B. Tian, H.F. Xiang, L. Zhang, Z. Li and H.H. Wang, *Electrochim. Acta*, 55 (2010) 5453.

30. Z.J. Yu, X.F. Zhang, G.L. Yang, J. Liu, J.W. Wang, R.S. Wang and J.P. Zhang, *Electrochim. Acta*, 56 (2011) 8611.
31. G.R. Hu, X.L. Zhang and Z.D. Peng, Trans. *Nonferrous Met. Soc. China*, 21 (2011) 2248.
32. J.Y. Lin, C.C. Hsu, H.P. Ho and S.H. Wu, *Electrochim. Acta*, 87 (2013) 126.
33. Y.J. Bai, C. Gong, N. Lun and Y.X. Qi, *J. Mater. Chem. A*, 1 (2013) 89.
34. B. Zhang, Z.D. Huang, S.W. Oh and J.K. Kim, *J. Power Sources*, 196 (2011) 10692.